Energy 65 (2014) 596–604

Contents lists available at ScienceDirect

Energy

journal homepage: www.elsevier.com/locate/energy

Aero-acoustics noise evaluation of H-rotor Darrieus wind turbines

M.H. Mohamed*

Renewable Energy Lab. of Mechanical Power Engineering Dept., Faculty of Engineering-Mattaria, Helwan University, P.O. 11718, Cairo, Egypt

A R T I C L E   I N F O

Article history:
Received 16 August 2013
Received in revised form
7 November 2013
Accepted 9 November 2013
Available online 8 December 2013

Keywords:
Wind energy
Noise
Darrieus turbine
Aerodynamic
CFD

A B S T R A C T

The problems aided with wind turbine noise have been one of the more studied environmental influence areas in wind energy engineering. Noise levels can be measured, but, similar to other environmental attentions, the public's perception of the noise impact of wind turbines is in part a subjective determination. The author investigated in this work the aerodynamic acoustics of one type of the VAWT (vertical axis wind turbine) which called Darrieus turbine. Darrieus turbine is suitable to be established within the densely populated city area. Therefore, the noise item is very important to investigate. In this work, Darrieus rotor has been studied numerically and aerodynamically to obtain the generated noise from blades. This work offers a method based on the FW–H (Ffowcs Williams and Hawkings) equations and its integral solutions. Time-accurate solutions can be obtained from URANS (unsteady Reynolds-averaged Navier–Stokes) equations. Blade shape, tip speed ratio and solidity effects have been studied in this work. The results indicated that the higher solidity and higher tip speed ratio rotors are more noisy than the normal turbines.

1. Introduction

Wind turbine generators, ranging in size from a few kilowatts to several megawatts, are producing electricity both singly and in wind power stations that involve hundreds of machines. Many installations are in uninhabited areas far from located residences, and therefore there are no visible environmental influences in terms of noise. There is, however, the potential for situations in which the radiated noise can be heard by residents of adjacent neighborhoods, particularly those neighborhoods with low ambient noise levels. Wind turbines noise frequency ranges from low values that sometimes inaudible to higher values in the normal audible range [1]. Although increased distance is advantageous in reducing noise levels, the wind can reinforce noise propagation in certain directions and prevent it in others. A unique feature of wind turbine noise is that it can result from basically continuous periods of daytime and nighttime operation. This is in disparity to the more common aircraft and road traffic noises that vary markedly as a function of time of day. The human ear comprehends loudness as an individual response to the amplitude of sound. At a given sound pressure level, the ear does not sense all frequencies to be of equal loudness. The normal hearing range of the human ear is 20 Hz–20 kHz, while the ear is most sensitive in the 3–4 kHz region [2].

Noise from wind turbines may be classified as aerodynamic or mechanical in origin. Aerodynamic noise components are either narrow-band (containing discrete harmonics) or broadband (random) and are related closely to the geometry of the rotor, its blades, and their aerodynamic flow environments. The low-frequency, narrow-band rotational components typically take place at the blade passage frequency (the rotational speed times the number of blades) and integer multiples of this frequency. Of lesser importance for most configurations are mechanical noise components from the operating bearings, gears, and accessories [3].

2. Noise propagation

Wind turbine generated Aerodynamic noise is still a considerable area of research. It is thought that aerodynamic (or aero-acoustic) noise from the blades emerges from a number of different mechanisms that are related to the way in which the flow over the airfoil interacts with the surrounding air. Techniques for prediction of the noise realized by an airfoil are usually based on theoretical principles but use empirically derived components to attain better agreement with what is observed in practice. Research into the reduction of aerodynamic noise from wind turbines has mainly concentrated on the use of serrated trailing edges, different trailing edge and tip shapes, and different airfoil profiles. The environmental aspects of wind turbine noise attach to how it

* Tel.: +20 112 6060 364; fax: +202 2633 2398.
E-mail addresses: mohamed_ibrahim07@m-eng.Helwan.edu.eg, moh75202@yahoo.de.

0360-5442/$ – see front matter © 2013 Elsevier Ltd. All rights reserved.
http://dx.doi.org/10.1016/j.energy.2013.11.031

propagates over the terrain surrounding the wind turbine and to how the noise is interpreted by people. The noise produced by wind turbines is often dashing and tonal, both of which can add to the annoyance factor of the sound. Several standards for calculation of the propagation of the sound are widely used and range from basic calculations that assume hemispherical propagation (see Fig. 1), to complex calculations designed to be done computationally which take into account the influences of terrain shape, barriers, wind speed and direction, atmospheric temperature profile, humidity, and air and ground absorption. A knowledge of the manner in which sound propagates through the atmosphere is basic to the process of predicting the noise fields of single and multiple machines. Although much is known about sound propagation in the atmosphere, the least understood factors are the impacts of distance from various types of sources, the effects of such atmospheric factors as absorption in air and refraction caused by sound speed gradients, and terrain effects. In this paper the author discusses numerically the intensity of the sound waves and the rate of decay of these waves.

3. Purpose of the present work

Many analytical and experimental acoustical studies performed the HAWTs (horizontal axis wind turbines). The results indicated that HAWTs with downwind rotors will generate more noise than will those with upwind rotors. This is because an additional noise source in downwind rotors is introduced when the rotating blades interact with the aerodynamic wake of the supporting tower.

The actual annoyance caused by a noise, is often a function of both the nature of the noise itself and a number of physiological factors. Studies conducted in Sweden on the leverages of wind power [4,5] detected a correlation between the general attitude of a person towards wind power and their level of annoyance. For example, a shareholder in a turbine may find the noise from it reassuring rather than annoying, whereas a summer resident who has gone to the countryside seeking peace and quiet would probably find it more of a disturbance. Pederson's [5] found that the most annoying noise heard from wind turbines was a swishing noise, followed by whistling and then pulsating and throbbing noises. It was also noted that the percentage of people annoyed increased as the noise levels increased. Pure wind turbine noise gave very similar annoyance ratings as unmixed highway noise at the same equivalent level, while annoyance by local road traffic noise was significantly higher [6].

Göçmena and özerdema focused on the optimization of six airfoils which are widely used on small scale wind turbines in terms of the noise emission and performance criteria and the numerical computations are performed for a typical 10 kW wind turbine. The main purpose of this optimization process was to decrease the noise emission levels while increasing the aerodynamic performance of a small scale wind turbine by adjusting the shape of the airfoil. The results obtained from the numerical analysis of the optimization process have shown that, the considered commercial airfoils for small scale wind turbines are improved in terms of aeroacoustics and aerodynamics. The pressure sides of the baseline airfoils have been manipulated together with the trailing edge and redesigned airfoils have lower levels of noise emission and higher lift to drag ratios [7].

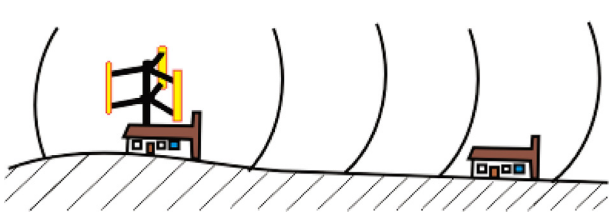

Fig. 1. Wind turbine noise propagation.

Obviously, noise is an impact factor that must be treated seriously and adequately, but it is only a secondary factor as far as attitudes are concerned. But it is established clear relations between experimental exposure to turbine noise and perceived annoyance [8,9].

Exploration of survey results showed individuals with a more negative attitude to wind turbines perceive more noise from a turbine located close to their dwelling and those perceiving more noise report increased levels of general symptoms. Individuals' personality also affected attitudes to wind turbines, noise perception from small and micro turbines and symptom reporting [10].

Conversely, the noise conspicuous to a listener could actually be increased under certain conditions. For example in the situation where the wind turbine is on a hill and the receptor site is somewhere at the base of the hill screened from the wind, the wind speed on top of the hill is likely to be 1.5:2 times the wind speed at the receptor site. This would reduce the background noise at the receptor site, and the wind turbine noise would thus appear to be more outstanding [11]. Application to a wind park shows clearly the influence of the terrain on the wind velocity and consequently on the SPL [12].

Rogers and Omer found that a doubling of the turbulence intensity from 0.3 to 0.6 resulted in an almost doubling of the sound energy level [13].

The results emphasized the hypothesis that the spectrum of wind turbine noise moves down in frequency with increasing turbine size. The relative amount of emitted low-frequency noise is higher for large turbines (2.3–3.6 MW) than for small turbines ($\leq$2 MW). The difference is statistically worth for one-third-octave bands in the frequency range 63–250 Hz. The difference can also be expressed as a downward shift of the spectrum of approximately one third of an octave [14]. At high rotational speeds the turbines produce a 'thumping', impulsive sound, increasing annoyance further [15].

The security level observed due to the wind turbine operation tends to increase with the increment of installed capacity. The social risk was calculated (characteristically arbitrary). As observed by the results (the curves in the F–N diagram) obtained for both scenarios, the risk does not exceed the upper limit of ALARP (as low as reasonably practicable) criterion. Nonetheless, the required application of principles for the integration of safety to tackle the hazards linked with wind turbines must not be neglected. Safety must be increased as the wind energy production expands, as well as there should be a need for regular reconsideration [16].

Comparison of the noise from the individual blades shows that the tripped blade is significantly noisier than the other two. Narrowband analysis of the de-dopplerized blade noise spectra indicates that trailing edge bluntness noise is not important. All in all, the test results convincingly show that broadband trailing edge noise is the dominant noise source for this wind turbine [17].

Because very little information on the acoustics of VAWTs (vertical axis wind turbines) is currently available, it is difficult to directly compare the noise generation characteristics of HAWTs and VAWTs [3].

The blades of a VAWT interact with the aerodynamic wake of the rotor's central column in a manner similar to the way that a downwind HAWT rotor interacts with its tower wake, but at a greater distance relative to the column diameter. Thus, the magnitude of the noise from a VAWT rises by this interaction. This is expected to be less than that of an equivalent downwind HAWT rotor and greater than that of an upwind HAWT rotor. There is currently no detailed information available describing other aerodynamic noise sources associated with VAWTs [3]. Thus, to gain an understanding of the acoustics of this type of turbine, additional studies are needed.

Therefore, the objectives of this work are (i) to investigate the main parameters affecting the aero-acoustics of Darrieus rotor; (ii) to assess our current ability to accurately predict corresponding turbine noise. The achievement of these objectives would enable quieter Darrieus wind turbines to be developed and allow them to be located in the domestic usage near residential dwellings with higher confidence that the noise would not be a nuisance.

4. Acoustics model theory

ANSYS-FLUENT presents three approaches to computing sounds, a direct method, an integral method based on acoustic analogy and a method that utilizes broadband noise source models. In this paper, the integral method based on acoustic analogy has been used because it is applicable only to predicting the propagation of sound toward open areas.

4.1. Integral method based on acoustic analogy

The main challenge in numerically predicting sound waves repels from the well-recognized fact that sounds have much lower energy than fluid flows, typically by several orders of magnitude. This poses a great challenge to the computation of sounds in terms of difficulty of numerically resolving sound waves, especially when one is interested in predicting sound propagation to the far field. Another challenge takes place from the difficulty of predicting the turbulence flow phenomena in the near field that are responsible for generating sounds. The accurate solution of the noise problem is strongly influenced by the unsteadiness of the rotor flow field, the nonuniform inflow effects and the blade aerodynamic parameters which are included in the numerical model [18].

This work offers a method based on the FW–H (Ffowcs Williams and Hawkings) equations and its integral solutions [19,20]. The FW–H formulation espouses the most general form of Lighthill's acoustic analogy [21], and is capable of predicting sound generated by equivalent acoustic sources, for instant, Darrieus turbine. ANSYS-FLUENT adopts a time-domain integral formulation wherein time histories of sound pressure generated form the turbine, or acoustic signals, at prescribed receiver locations are directly computed by estimating a few surface integrals. Time-accurate solutions of the flow-field variables around the turbine, such as pressure, velocity components, and density on source surfaces, are required to evaluate the surface integrals. Time-accurate solutions can be obtained from URANS (unsteady Reynolds-averaged Navier–Stokes) equations. The source surfaces can be placed not only on impermeable walls, but also on interior surfaces, which authorizes you to account for the contributions from the quadrupoles enclosed by the source surfaces. The FW–H acoustics model in FLUENT permits you to select multiple source surfaces and receivers. It also allows you either to save the source data for a future use, or to implement an "on the fly" acoustic calculation simultaneously as the transient flow calculation proceeds, or both. Sound pressure signals thus obtained can be processed using the FFT (fast Fourier transform) and associated postprocessing capabilities to compute and plot all acoustic quantities [23].

4.2. The Ffowcs Williams and Hawkings model

The FW–H (Ffowcs Williams and Hawkings) equation is basically an inhomogeneous wave equation that can be obtained by manipulating the continuity equation and the Navier–Stokes equations. The FW–H [19,22,23] equation can be written as:

$$\frac{1}{a_o^2}\frac{\partial^2 p'}{\partial t^2} - \nabla^2 p' = \frac{\partial^2}{\partial x_i \partial x_j}\{T_{ij}H(f)\} - \frac{\partial}{\partial x_i}\{[P_{ij}n_j + \rho u_i(u_n - v_n)]\,\delta(f)\} + \frac{\partial}{\partial t}\{[\rho_o v_n + \rho(u_n - v_n)]\delta(f)\} \tag{1}$$

where

u_i = fluid velocity component in the x_i direction
u_n = fluid velocity component normal to the surface $f = 0$
v_i = surface velocity components in the x_i direction
v_n = surface velocity component normal to the surface
$\delta(f)$ = Dirac delta function
$H(f)$ = Heaviside function

p' is the sound pressure at the far field ($p' = p - p_0$). $f = 0$ denotes a mathematical surface introduced to "embed" the exterior flow problem ($f > 0$) in an unbounded space, which facilitates the use of generalized function theory and the free-space Green function to obtain the solution. The surface ($f = 0$) corresponds to the source (emission) surface (blades and shaft). n_i is the unit normal vector pointing toward the exterior region ($f > 0$), a_0 is the far-field sound speed, and T_{ij} is the Lighthill's stress tensor [23], defined as

$$T_{ij} = \rho u_i u_j + P_{ij} - a_o^2(\rho - \rho_o)\delta_{ij} \tag{2}$$

P_{ij} is the compressive stress tensor. For a Stokesian fluid, this is given by

$$P_{ij} = p\delta_{ij} - \mu\left[\frac{\partial u_i}{\partial x_j} + \frac{\partial u_j}{\partial x_i} - \frac{2}{3}\frac{\partial u_k}{\partial x_k}\delta_{ij}\right] \tag{3}$$

Free-stream quantities are denoted by the subscript o.

The solution to Eq. (1) is obtained using the free-space Green function ($\delta(g)/4\pi r$). The whole solution consists of surface integrals and volume integrals. The surface integrals explain the contributions from monopole and dipole acoustic sources and partially from quadrupole sources, whereas the volume integrals represent quadrupole (volume) sources in the region outside the source surface. The contribution of the volume integrals becomes small when the flow is low subsonic as in the Darrieus turbine case. In FLUENT, the volume integrals are dropped [23]. Thus, we have

$$p'(\vec{x},t) = p'_T(\vec{x},t) + p'_L(\vec{x},t) \tag{4}$$

where

$$4\pi p'_T(\vec{x},t) = \int_{f=0}\left[\frac{\rho_o\left(\dot{U}_n + U_{\dot{n}}\right)}{r(1-M_r)^2}\right]ds + \int_{f=0}\left[\frac{\rho_o U_n\left\{r\dot{M}_r + a_o\left(M_r - M^2\right)\right\}}{r^2(1-M_r)^3}\right]ds \tag{5}$$

$$4\pi p'_L(\vec{x},t) = \frac{1}{a_o}\int_{f=0}\left[\frac{\dot{L}_r}{r(1-M_r)^2}\right]ds + \int_{f=0}\left[\frac{L_r - L_M}{r^2(1-M_r)^2}\right]ds + \frac{1}{a_o}\int_{f=0}\left[\frac{L_r\left\{r\dot{M}_r + a_o\left(M_r - M^2\right)\right\}}{r^2(1-M_r)^3}\right]ds \tag{6}$$

where

$$U_i = v_i + \frac{\rho}{\rho_o}(u_i - v_i) \quad (7)$$

$$L_i = P_{ij}\hat{n}_j + \rho u_i(u_n - v_n) \quad (8)$$

When the integration surface synchronizes with an impenetrable wall, the two terms on the right in Eq. (4), $p'_T(\vec{x}, t)$ and $p_L(\vec{x}, t)$, are often pointed out to as thickness and loading terms, respectively, in light of their physical meanings. The square brackets in Eqs. (5) and (6) mention that the kernels of the integrals are computed at the corresponding retarded times, τ, defined as follows, given the observer time, t, and the distance to the observer, r,

$$\tau = t - \frac{r}{a_o} \quad (9)$$

The various subscripted quantities appearing in Eqs. (5) and (6) are the inner products of a vector and a unit vector tacit by the subscript. For instance, $L_r = \vec{L} \cdot \widehat{\vec{r}} = L_i r_i$ and $U_n = \vec{U} \cdot \vec{n} = U_i n_i$, where $\vec{r}$ and $\vec{n}$ denote the unit vectors in the radiation and wall-normal directions, respectively. The dot over a variable announces source-time differentiation of that variable [23]. There are some remarks regarding the applicability of this integral solution:

(1) The FW–H formulation can treat rotating surfaces as well as stationary surfaces.
(2) It is not required that the surface $f = 0$ coincide with body surfaces or walls. The formulation allows source surfaces to be permeable, and therefore can be placed in the interior of the flow.
(3) When a permeable source surface (either interior or non-conformal sliding interface) is placed at a certain distance of the body surface, the integral solutions given by Eqs. (5) and (6) involve the contributions from the quadrupole sources within the region enclosed by the source surface. When using a permeable source surface, the mesh resolution needs to be fine enough to resolve the transient flow structures inside the volume enclosed by the permeable surface.

5. CFD methodology

CFD transacts with the numerical analysis of complex flows. regardless of impressive progress in recent years, CFD remains an imperfect tool in the comparatively mature discipline of fluid dynamics. Due to the highly time-dependent nature of the flow around the Darrieus rotor, the CFD simulation of a Darrieus turbine is a very difficult mission. It is therefore necessary to check the full numerical model with great care. Thereafter, the resulting methodology must be validated. ANSYS-FLUENT has been used in this work. Fluent is the world's leading commercial supplier of Computational Fluid Dynamics software and services. Unsteady Reynolds-Averaged Navier–Stokes equations have been solved using the SIMPLE algorithm for pressure–velocity coupling. Discretization has been preceded using the Finite-Volume method with second-order upwind scheme for all variables. Fig. 2 illustrates all the details about the boundary conditions and the computational domain.

5.1. Mesh generation

The unsteady flow is solved by using the SMM (Sliding Mesh Model). Four complete revolutions are always computed, the first one is used to initiate the correct flow solution, while the flow properties are obtained by averaging the results during the last three revolutions and the acoustic signals for all receivers (see Fig. 3) can be calculated and captured during instantaneously

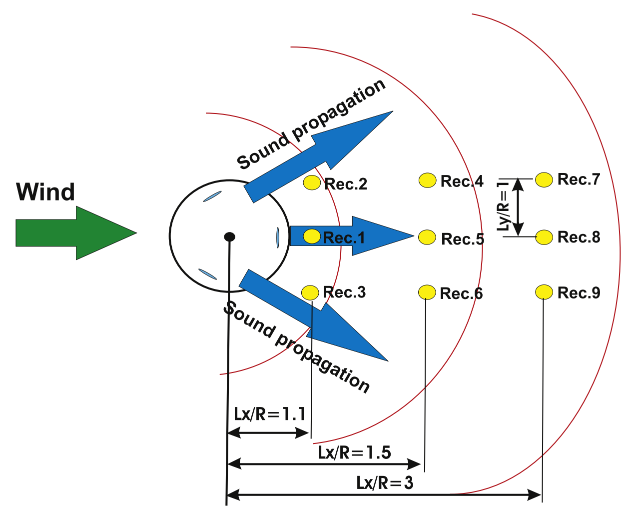

Fig. 3. Pressure wave propagation and the positioning of the receivers.

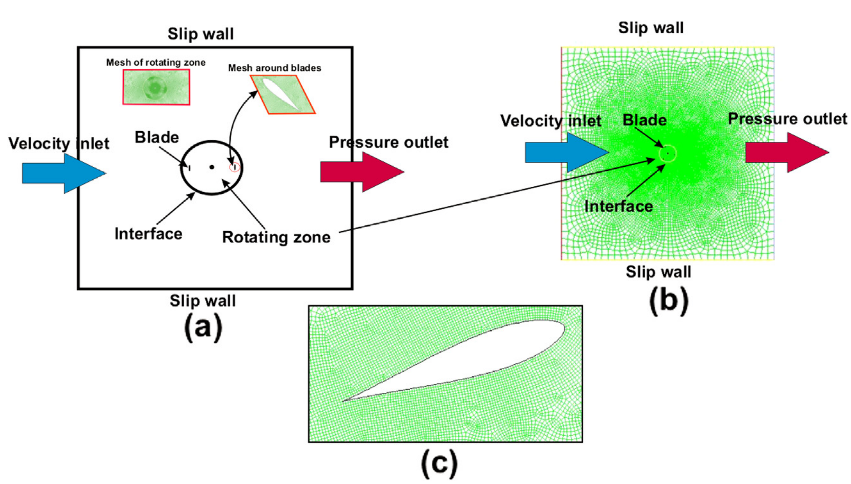

Fig. 2. CFD domain and sample of mesh around rotating zone and blade; b) Domain mesh; c) mesh around blade.

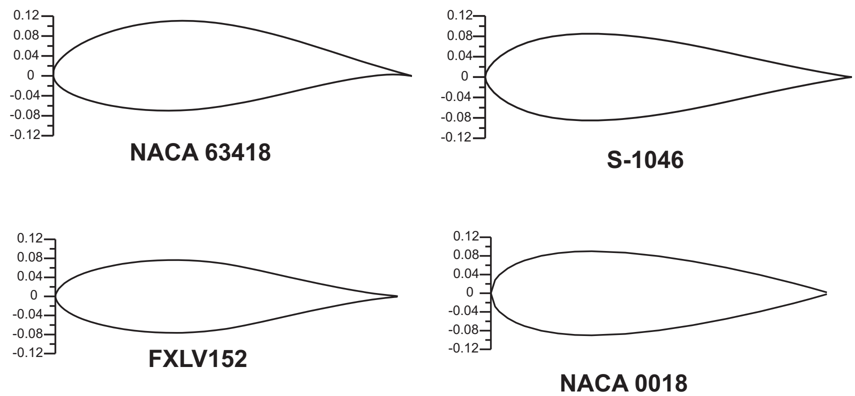

Fig. 4. Airfoil shapes included in the sound intensity comparison.

during the last revolution. The inlet velocity is retained as constant and equal 9 m/s and the pressure outlet is the atmospheric pressure (see Fig. 2). On a standard PC, one evaluation (i.e., four revolutions for one specific configuration) takes about 285 min of computing time. A mesh size independence test is accomplished for one geometrical configuration. Several different two-dimensional, unstructured grids of increasing density and quality, collected of different mesh size ranging from 6000 up to 135,000 cells are scanned. This test offers that more than 80,000 cells lead to a relative variation of the output quantity below 1.12%. The moderate grid range between 80,000 and 95,000 cells has been conserved for all further results due to the computing time. The adequate size of the computational domain has been studied [24]. Mohamed in Refs. [24,25] has recommended a new design for Darrieus turbine consists of s-1046 airfoils cross section.

5.2. Turbulence model validation

Numerical turbulence model validation is the second step in the CFD process after the mesh and domain independence studies. The validation comparison has been gained between the new model results and published experimental and CFD results for a H-rotor Darrieus turbine [24,25]. These results indicated an acceptable agreement between the experiments and present CFD for the target

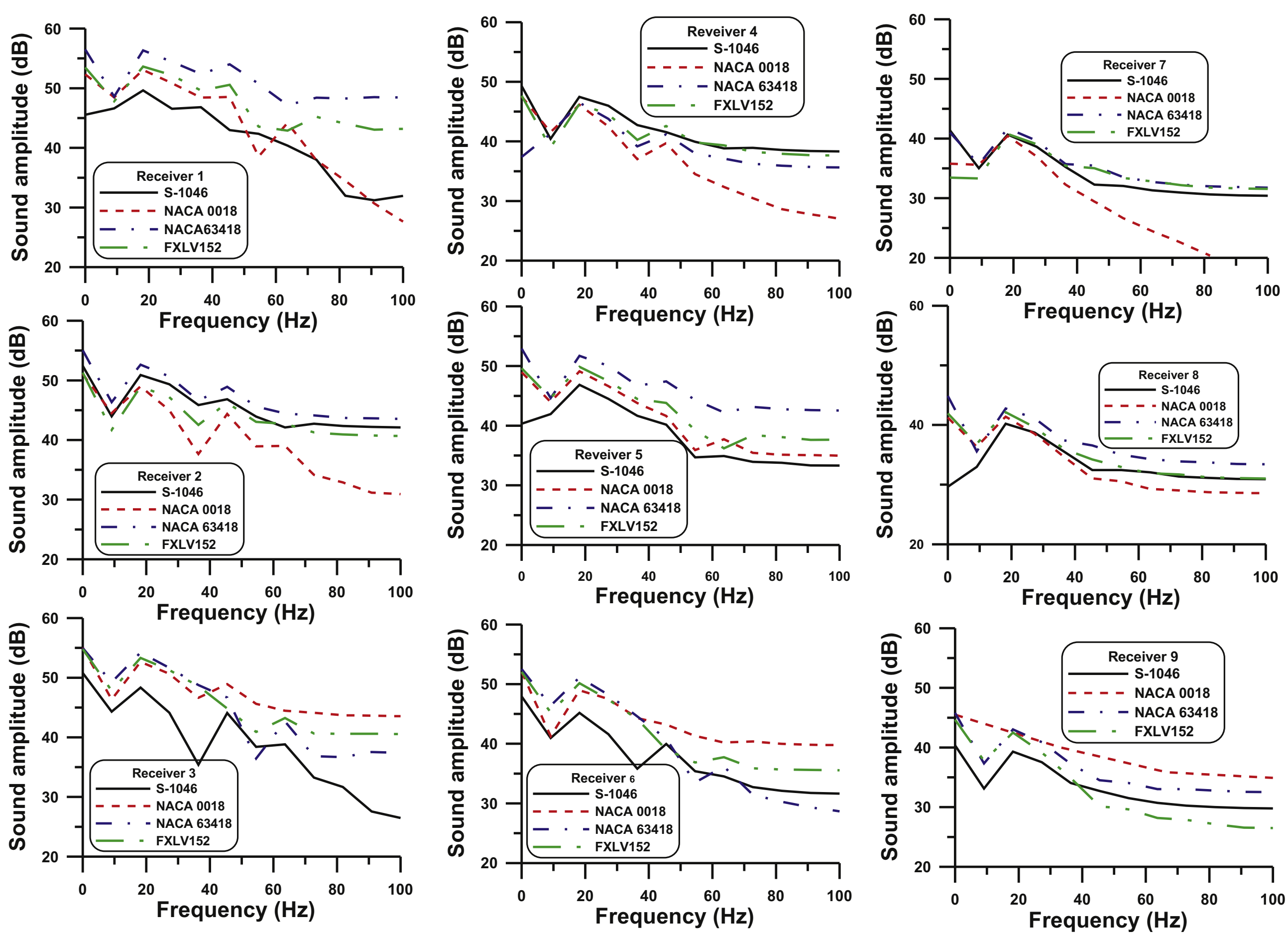

Fig. 5. Effect of the airfoil shape on the sound intensity.

function, C_p quantitatively and qualitatively by using the realizable k−ε turbulence model. Same trend has been observed for other studies encompassing rotating blades [26,27] and airfoils as in Refs. [28,29], proving the interest of the realizable k- model for fast CFD simulations. The realizable k−ε model is usually recommended for rotating bodies. Therefore, in this work the realizable k−ε turbulence model will be retained in all the aerodynamic simulation. The realizable k-ε turbulence model has been acquired by Shih et al. [30].

6. Results and discussion

There is currently no publications available describing other aerodynamic noise sources associated with Darrieus turbine. Thus, to gain an understanding of the acoustics of this type of turbine, additional studies are needed. Therefore, some effective parameters have been investigated in this work. For instant, the blade shape, the speed ratio, the solidity and the receiver distance form the turbine location. In the next sections, a discussion for these parameter results will be introduced.

6.1. Airfoil shape effect

Mohamed [28] studied the effect of the airfoil shape on the characteristics performance of the rotor; torque and power coefficients according to variables of airfoil blade shape. Twenty airfoil (symmetric and non-symmetric) have been investigated and the results indicated that the S-1046 is the best airfoil from the performance point of view. Therefore, in this work, the aeroacoustic of S-1046 has been studied and compared with another airfoils which have a good performance as NACA 0018, NACA 63418 and FXLV152 [28] as shown in Fig. 4. Sound intensities of these airfoils have been investigated as shown in Fig. 5. From the results, it has been concluded that the blade shape is very intersecting parameter in the noise generation. The results of the comparison introduced another advantage to S-1046 because it is less in the sound intensity at most of the receivers. Therefore, the author recommends the S-1046 airfoil for the H-rotor Darrieus turbine from two point of views; the high performance and the less noise generation.

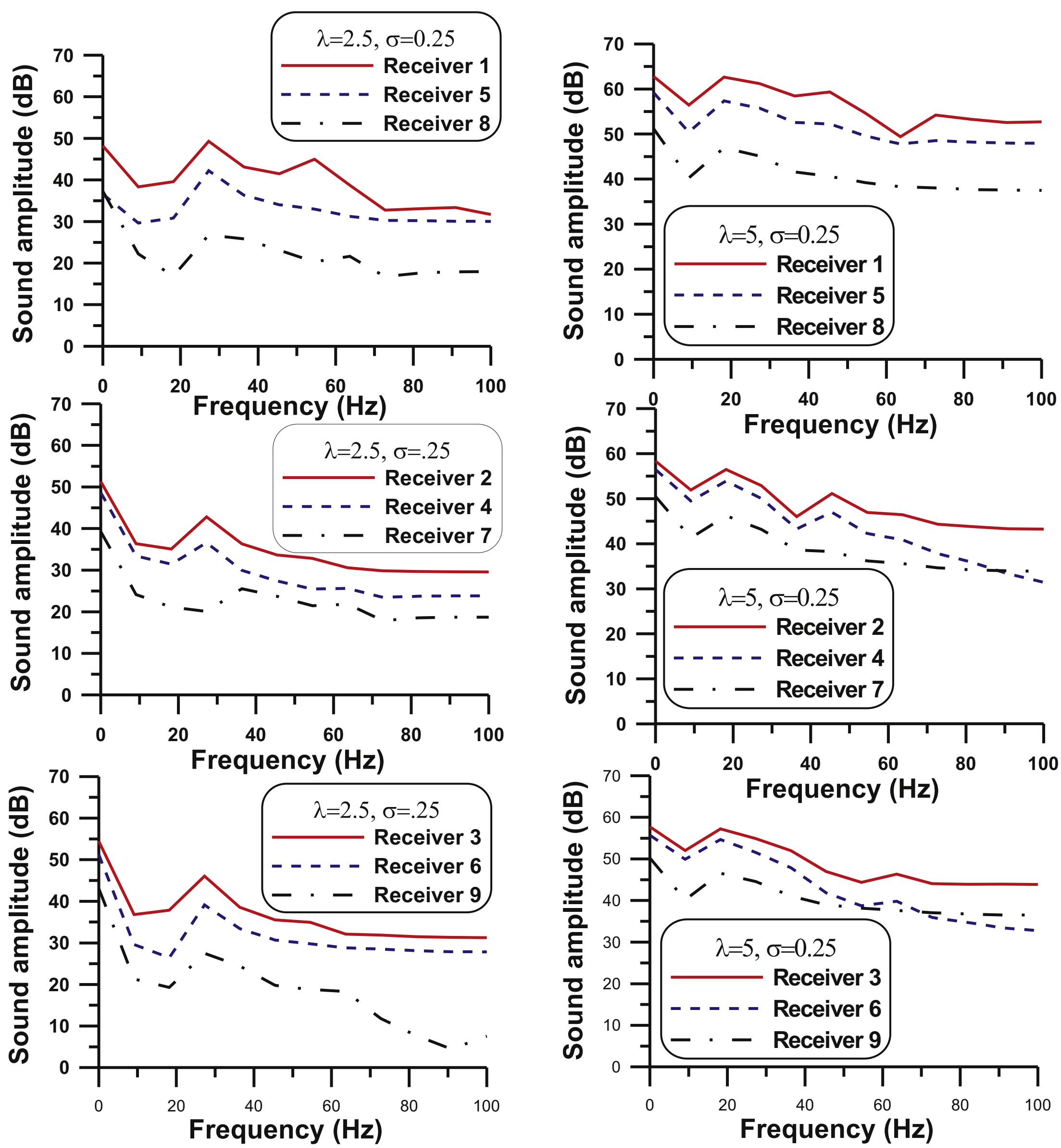

Fig. 6. Tip speed ratio effect on the noise generation of Darrieus turbine.

6.2. Speed ratio effect

The tip-speed ratio (λ) is a dimensionless number which can be defined as ($\lambda = \omega R/U$), where R is the rotor radius (m), ω is the rotating speed (rad/sec) and U is the flow velocity (m/s). In this section, the speed ratio effect on the turbine noise has been investigated. The results indicate that the increasing of the speed ratio increases the noise form Darrieus turbine as shown in Fig. 6. Two different speed ratios have been studied ($\lambda = 2.5$ and $\lambda = 5$) for the same turbine solidity ($\sigma = 0.25$). For all receivers the results suggested that the rotational speed should be small to reduce the noise generations. The average reduction of the sound amplitude is 17.3 dB, if the speed ratio decreases from $\lambda = 5$ to $\lambda = 2.5$. This reduction is a significant number especially in the residential areas.

6.3. Solidity effect

The proximity of the rotor blades affects the performance of the Darrieus turbine due to the aerodynamic interferences losses [24]. The performance of a H-rotor Darrieus turbine rotor is subjected to mutual aerodynamic interaction between the blades. The mutual aerodynamic interaction is due to the wakes produced by the blades. This interaction is a function of air flow incident and solidity of the blades $\sigma = nc/2R$. Due to this wake effect, the angle of attack will be larger leading to an earlier blades stalling and decreases the aerodynamic efficiency of these blades and this leads to earlier separation and generates some eddies which gives some noise. In this section, the solidity effect of the H-rotor Darrieus turbine on the sound generation is investigated. The sound amplitude at two different solidities ($\sigma = 0.1$ and $\sigma = 0.25$) are studied and the results indicated that the sound level will increase with increasing the solidity (see Fig. 7). Form the results, the increasing of the solidity from 0.1 to 0.25 increases the noise emissions by 7.6 dB.

6.4. Effect of distance between the source and receivers

When there is a point source or multiple point sources, spherical spreading may be assumed in the far radiation field. Circular wave fronts propagate in all directions from a point source, and the sound levels decay at the rate of 5.86 dB per unit of (L_x/R); the distance of the receiver from the source. It is noted that the average decay rate is approximately constant. From this reduction rate, sound vanishing distance ratio (L_x/R) is calculated as 9.53. Fig. 8 illustrates the rate of decay of the noise radiation for different frequencies and different solidities.

7. Conclusions

VAWT (Vertical Axis Wind Turbines) like the Darrieus turbine appear to be particularly promising for the conditions of low wind

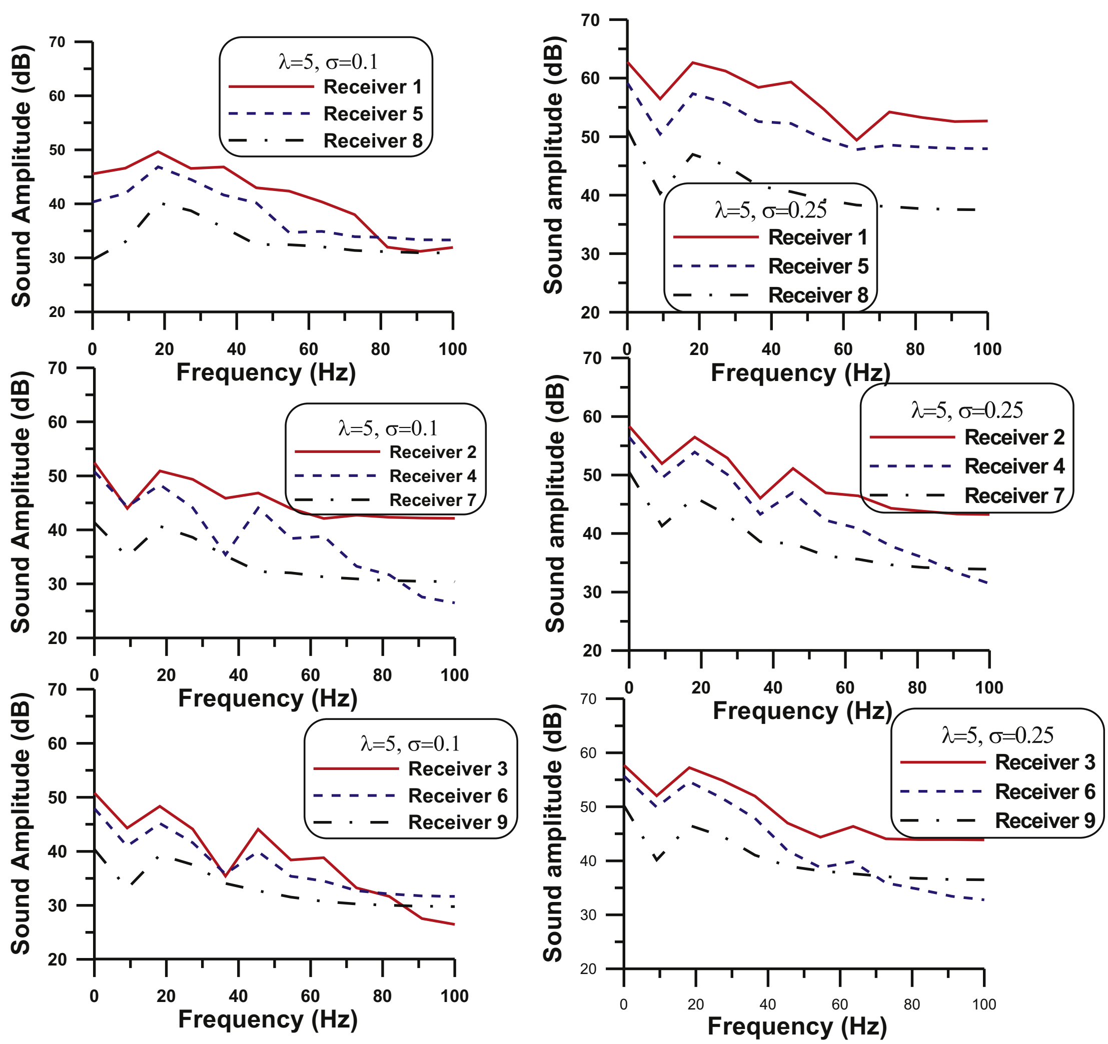

Fig. 7. Darrieus turbine solidity effect on the noise generation.

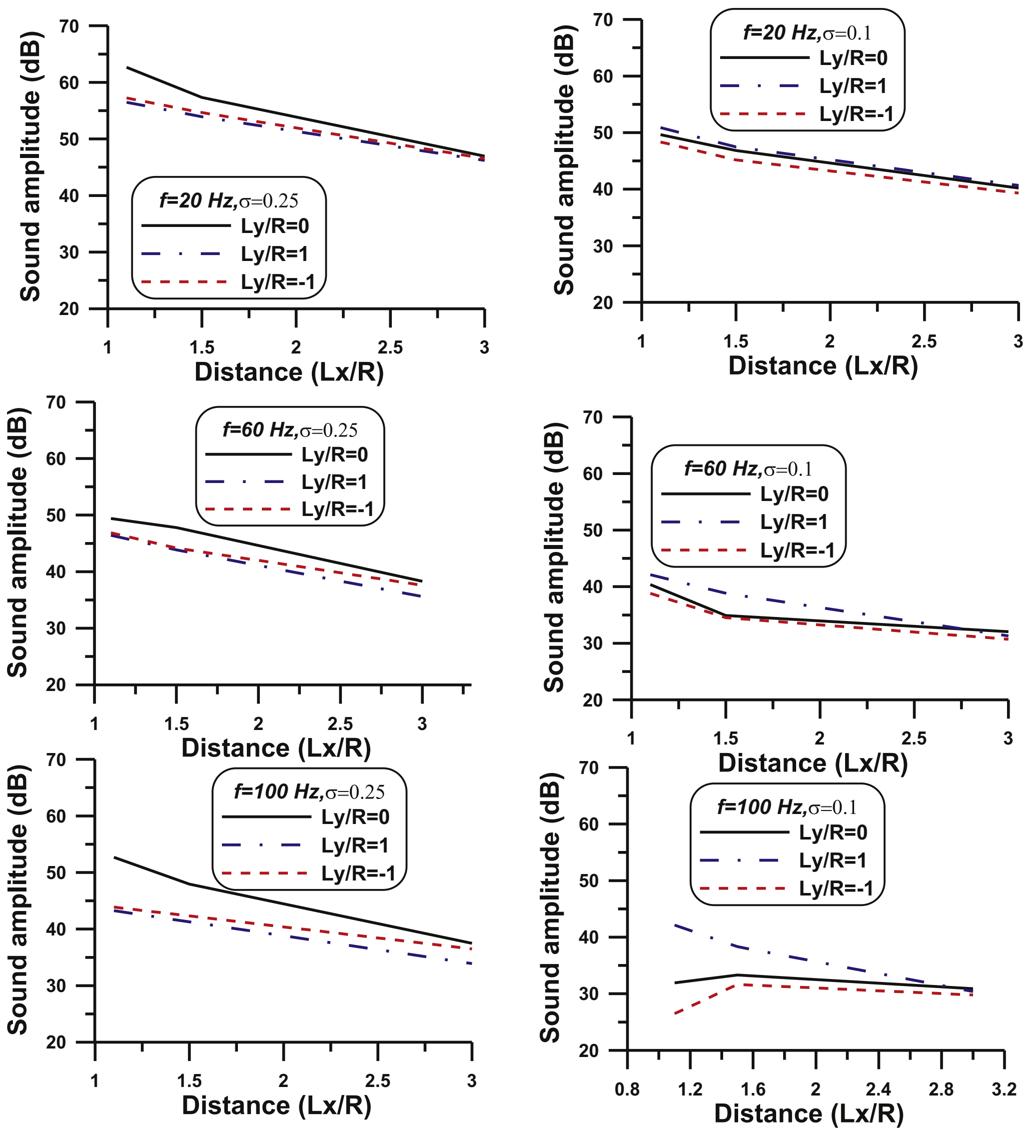

Fig. 8. Effect of Distance between the source and receivers.

speed. There is currently no detailed information available describing other aerodynamic noise sources associated with VAWTs. Thus, to gain an understanding of the acoustics of this type of turbines, this work has been introduced. This work uses a method based on the Ffowcs Williams and Hawkings (FW–H) equations. These equations are recommended for the rotating zones and sliding mesh model. Ffowcs Williams and Hawkings (FW–H) model has been implemented in ANSYS-FLUENT, therefore, all the results in this work have been calculated by the commercial CFD program ANSYS-FLUENT. The effect of the blade shape, the speed ratio, solidity and the distance between the noise source (Darrieus turbine) and the receivers are investigated in this work. S-1046 is the best airfoil from the noise point of view due to less aerodynamic noise generation. In addition, the results indicated that increasing the tip speed ratio increases the noise generated form Darrieus turbine. Moreover, the decreasing of the solidity reduces the noise emission from the turbine by 7.6 dB if the solidity is reduced from 0.25 to 0.1. However, the average of the noise decay rate is 5.86 dB per every unit of (L_x/R) from the distance between the turbine and the receivers. Finally, the author is believing that work is unique in noise emissions field especially for Darrieus turbine.

Acknowledgments

The Post-doctor work of Dr. Mohamed is supported financially by a bursary of the DAAD. The author would like to thank Prof. Dominique Thévenin the head of Laboratory of Fluid Dynamics and Technical Flows University of Magdeburg "Otto von Guericke" Magdeburg, Germany, for his help.

References

[1] Kelley ND, McKenna HE, Hemphill RR, Etter CL, Garrelts RC, Linn NC. Acoustic noise associated with the MOD-1 wind turbine: its source, impact and control. SERI TR-635–1166. Golden, Colorado: Solar Energy Research Institute; Feb. 1985.
[2] Robinson D, Dadson R. A re-determination of equal loudness relations for pure tones. Br J Appl Acoust 1956;7:166–81.
[3] Hubbard HH, Shepherd KP. Wind turbine acoustics; 1990. NASA Technical Paper 3057 DOE/NASA/20320–77.
[4] Hammarlund K. The social impacts of wind power. In: Presented at EWEA conference, Goteborg, Sweden 1997.
[5] Pedersen E, Persson Waye K. The impact of wind turbines in Sweden with special reference to noise annoyance. In: Presented at EWEA conference, Copenhagen, Denmark 2001.
[6] Van Renterghem Timothy, Bockstael Annelies, Weirt Valentine De, Botteldooren Dick. Annoyance, detection and recognition of wind turbine

noise. Original Research Article Sci Total Environ 1 July 2013;456–457:333–45.
[7] Göçmen T, özerdem B. Airfoil optimization for noise emission problem and aerodynamic performance criterion on small scale wind turbines. Original Research Article Energy 2012;46(1):62–71.
[8] Wolsink M. Wind power implementation: the nature of public attitudes: equity and fairness instead of 'backyard motives'. Renew Sustain Energy Rev 2005:1188–207.
[9] Devine-Wright P. Beyond NIMBYism: towards an integrated framework for understanding public perceptions of wind energy. Wind Energy 2005:125–39.
[10] Taylor Jennifer, Eastwick Carol, Lawrence Claire, Wilson Robin. Noise levels and noise perception from small and micro wind turbines. Original Research Article Renew Energy July 2013;55:120–7.
[11] Theofiloyiannakos D, Zorlos P, Agoris D. Current practices for the prediction and assessment of the environmental impact from wind energy projects in Greece. In: Presented at EWEA conference, Copenhagen, Denmark 2001.
[12] Prospathopoulos JM, Voutsinas SG. Application of a ray theory model to the prediction of noise emissions from isolated wind turbines and wind parks. Wind Energy 2007:103–19.
[13] Rogers T, Omer S. The effect of turbulence on noise emissions from a micro-scale horizontal axis wind turbine. Original Research Article Renew Energy May 2012;41:180–4.
[14] Henrik M, Christian SP. Low-frequency noise from large wind turbines. Acoust Soc Am 2011:3727–44.
[15] Van Den Berg GP. Effects of the wind profile at night on wind turbine sound. J Sound Vib 2004:955–70.
[16] Moura Carneiro FO, Barbosa Rocha HH, Costa Rocha PA. Investigation of possible societal risk associated with wind power generation systems. Renew Sustain Energy Rev 2013:30–6.
[17] Oerlemans S, Sijtsma P, Méndez López B. Location and quantification of noise sources on a wind turbine. J Sound Vib 2007:869–83.
[18] Filios AE, Tachos NS, Fragias AP, Margaris DP. Broadband noise radiation analysis for an HAWT rotor. Renew Energy 2007:1497–510.
[19] Ffowcs-Williams JE, Hawkings DL. Sound generation by turbulence and surfaces in arbitrary motion. Proc Roy Soc Lond 1969;A264:321342.
[20] Tadamasa A, Zangeneh M. Numerical prediction of wind turbine noise. Original Research Article Renew Energy July 2011;36(7):1902–12.
[21] Lighthill MJ. On sound generated aerodynamically. Proc Roy Soc Lond 1952;A211:564587.
[22] Brentner KS, Farassat F. An analytical comparison of the acoustic analogy and Kirchhoff formulations for moving surfaces. AIAA J 1998;36(8).
[23] Fluent Inc. Fluent 6.3.26 user's guide. Fluent Inc; 2005.
[24] Mohamed MH. Performance investigation of H-rotor Darrieus turbine with new airfoil shapes. Energy 2012;47(1):522–30.
[25] Mohamed MH. Impacts of solidity and hybrid system in a small wind turbine performance. Energy 2013;57(8):495–504.
[26] Mohamed MH, Janiga G, Pap E, Thévenin D. Optimization of Savonius turbines using an obstacle shielding the returning blade. Renew Energy 2010;35(11):2618–26.
[27] Mohamed MH, Janiga G, Pap E, Thévenin D. Optimal blade shape of a modified Savonius turbine using an obstacle shielding the returning blade. Energy Convers Manage 2011;52(1):236–42.
[28] Mohamed MH, Janiga G, Pap E, Thévenin D. Multi-objective optimization of the airfoil shape of wells turbine used for wave energy conversion. Energy 2011;36(1):438–46.
[29] Mohamed MH, Shapaan S. Optimization of blade pitch angle of an axial turbine used for wave energy conversion. Energy 2013;56(7):229–39.
[30] Shih T, Liou WW, Shabbir A, Yang Z, Zhu J. A new k- eddy viscosity model for high Reynolds number turbulent flows. Comput Fluids 1995;24(3):227–38.

Nomenclature

A: projected area of rotor (DH), m^2
C_p: power coefficient ($P/[1/2\rho AU^3]$)
c: blade chord, m
D: turbine diameter ($2R$), m
H: blade height, m
N: rotational speed of rotor, rpm
n: number of blades
R: radius of turbine, m
U: mean wind velocity in axial direction, m/s
u: peripheral velocity of the blade, m/s
σ: solidity, ($nc/2R$)
λ: speed ratio, ($\omega R/U$)
ρ: density, kg/m^3
ω: angular speed, 1/s